Angular Momentum in Terms of Toroidal and Poloidal Stream Functions

Loren Matilsky

November 8, 2022

1 Prior Work Considered

In this set of notes, we consider 3D nonlinear dynamo simulations that explored magnetic-field amplitudes at a variety of rotation rates (i.e., enough to make scatter plots of various quantities versus Rossby number and thus theoretically address the activity-rotation relation). We aim to determine what region of parameter space has been explored by global models, and in particular, how the rotation-activity relation may or may not have been addressed. The works considered are:

Christensen & Aubert (2006),

Christensen et al. (2009),

Strugarek et al. (2017),

Guerrero et al. (2019),

Brun et al. (2022),

2 Observations of the Stellar Activity-Rotation Relation (ARR)

The stellar activity-rotation relation (hereafter ARR) has a long history of observation and informs astronomers' generally accepted picture of stellar spin-down. The positive correlation between rotational velocity ($v \sin i$) and chromospheric Ca^+ emission (more or less considered to be linearly proportional to strength of the surface magnetic field) was first noted by Kraft (1967). This correlation was made famous in the context of spin-down by the "Skumanich $t^{1/2}$" law. This law states that as a star ages (call its age t), its surface magnetic-field strength and rotation rate both decrease like $t^{-1/2}$ (Skumanich 1972). Since spin-down is believed to be caused by angular-momentum loss from a stellar wind, there thus appears to

be a negative feedback loop between rotation (which produces magnetic field by a convective dynamo) and magnetic field (which drives the stellar wind and slows the rotation).

In addition to chromospheric emission, coronal emission (X-ray luminosity) is also found to be proportional to the rotation rate (e.g., Walter 1982). Furthermore, the X-ray data show that for a critical rotation rate (corresponding to a critical mixing-length Rossby number of $Ro \sim 0.1$), the ratio of X-ray luminosity to total luminosity saturated to a value of $L_X/L_* \sim 0.001$. It is still unclear whether this saturation regime corresponds a fundamental dynamo process (for example, the inability of the dynamo to convert additional kinetic energy to magnetic field) or simply geometric effects (for example, the stellar surface becoming so peppered with active regions that it cannot accommodate any more dynamo-produced flux) (Jardine & Unruh 1999). More recent work (Reiners et al. 2022) claims that the saturation regime indicates a fundamental dynamo process.

Since the detailed properties of the magnetic fields in stellar interiors are almost completely unconstrained (including for the Sun), it is reasonable to assume that the overall dynamo strength (defined here to be the rms magnetic-field strength, with the mean taken over the full volume of the star) is proportional to the surface magnetic-field strength, and thus to the proxies of Ca^+ and X-ray flux. With these assumptions, the ARR tells us about two stellar dynamo regimes: slow rotation (where the Sun lies), in which dynamo strength increases with more rapid rotation, and fast rotation, in which the dynamo strength is insensitive to the rotation rate (a saturation regime). Figure 2 shows the ARR as reported by Reiners et al. (2022). As the Rossby number Ro (ratio of well-measured rotation period $P_{\rm rot}$ to an ad hoc convective turnover time τ) decreases right to left (i.e., the rotation rate increases), the surface magnetic field strength increases up to a critical Rossby number $Ro = 0.13$. After that, faster rotation only leads to marginally increased field strength.

It should be noted that the "Rossby number" used in plots like Figure 2 is really an empirical parameter chosen to make the ARR collapse onto a single curve for all different stellar masses (e.g., Noyes et al. 1984; Pizzolato et al. 2003; Wright et al. 2011). In general, the empirical convective turnover time scales like $\tau \sim L_*^{1/2}$, which has some basis in mixing-length theory, but the true dependence of τ on stellar parameters could be far more complicated. In any case, simply plotting the normalized activity emission (e.g., L_X/L_*) with respect to rotation period yields an essentially similar ARR, possibly with different saturation breaks (all in the range of $P_{\rm rot} \sim$ 1–3 days) for different stellar masses (e.g., Pizzolato et al. 2003).

3 Parameters Spaces Explored

Global, rotating, magnetized spherical shells are characterized by several non-dimensional parameters. These parameters (which completely characterize the Boussinesq system) are:

$$\text{shell aspect ratio} \quad \equiv \quad \beta \quad \equiv \quad \frac{r_{\rm i}}{r_{\rm o}}, \tag{1}$$

$$\text{Rayleigh number} \quad \equiv \quad {\rm Ra_B} \quad \equiv \frac{g_{\rm o}\alpha\Delta\overline{T}}{\nu_{\rm o}\kappa_{\rm o}H^5}, \tag{2}$$

$$\text{thermal Prandtl number} \quad \equiv \quad {\rm Pr} \quad = \quad \frac{\nu_{\rm o}}{\kappa_{\rm o}}, \tag{3}$$

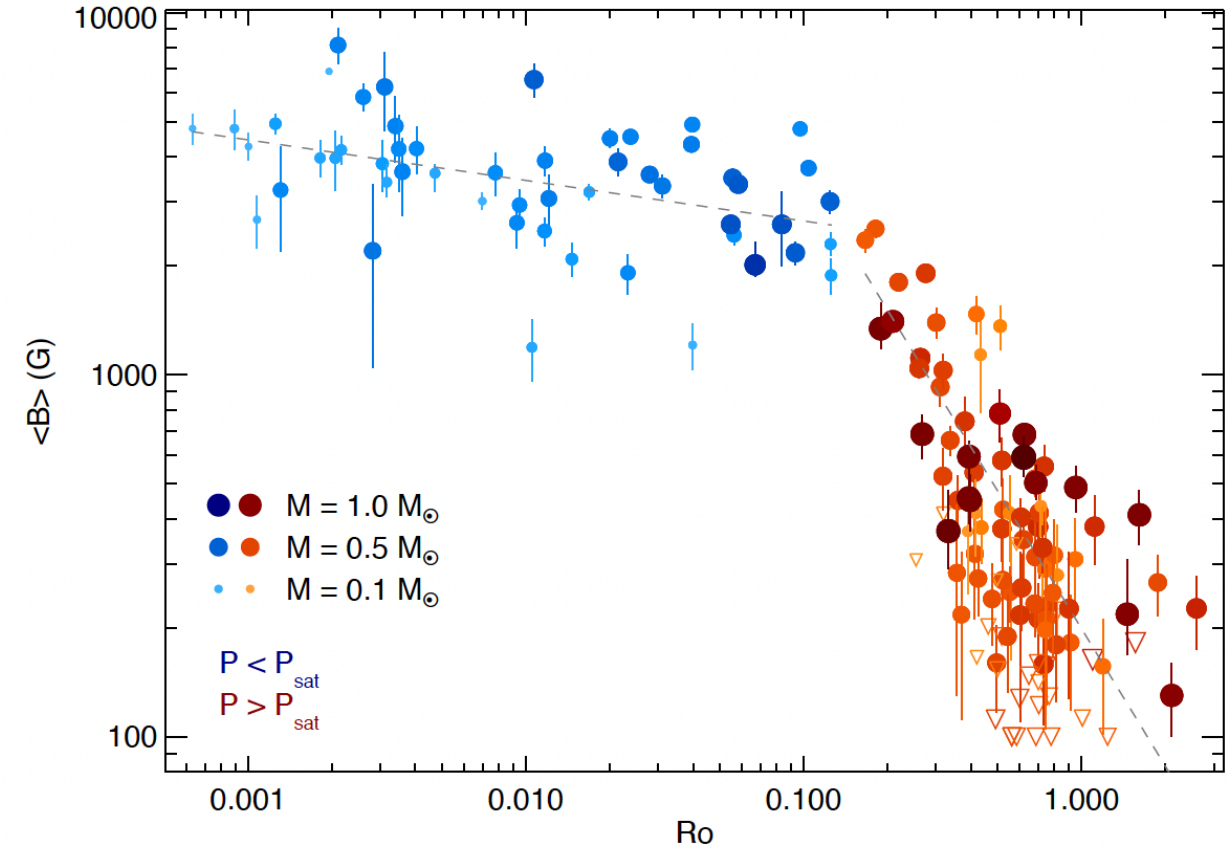

Figure 1: Copied from Reiners et al. (2022), Figure 5: Magnetic field–rotation relation for solar-like and low-mass stars. Symbols for stars rotating slower than $Ro = 0.13$ are colored red, while those of faster rotators are colored blue. Larger and darker symbols indicate higher stellar mass than smaller and lighter symbols. The gray dashed lines show linear fits separately for the slowly rotating stars ($Ro > 0.13$; $\langle B \rangle = 200G \times Ro^{-1.25}$) and the fast rotators ($Ro < 0.13$; $\langle B \rangle = 2050G \times Ro^{-0.11}$). Downward open triangles show upper limits for $\langle B \rangle$.

$$\text{Ekman number} \quad \equiv \quad \text{Ek} \quad = \frac{\nu_\text{o}}{\Omega_0 H^2}, \tag{4}$$

$$\text{and} \quad \text{magnetic Prandtl number} \quad \equiv \quad \text{Pr}_\text{m} \quad = \quad \frac{\nu_\text{o}}{\eta_\text{o}}. \tag{5}$$

Here, r is the radius, the subscripts "o" and "i" refer to the outer and inner radii of the shell (respectively), $H = r_\text{o} - r_\text{i}$ is the shell depth, g is the gravitational acceleration, α is the coefficient of thermal expansion, $\Delta\overline{T}$ is the background (superadiabatic, or adverse) temperature difference between the bottom and top of the shell, ν is the kinematic viscosity, κ the thermal diffusivity, Ω_0 the rotation rate, and η the magnetic diffusivity. The "o" subscripts on the diffusivities and g indicate they are in general functions of r. Technically, this radial dependence makes the parameter space accessed by dynamo simulations infinite-dimensional, so hopefully it's not too important! Just kidding.

If the system is anelastic, there are additional parameters because of the stratification. For a polytrope describing a convection zone, these are:

$$\text{shell density contrast} \quad \equiv \quad \text{DC} \quad \equiv \frac{\overline{\rho}(r_\text{i})}{\overline{\rho}(r_\text{o})} \tag{6}$$

$$\text{or} \quad \text{number of density scale heights} \quad \equiv \quad N_\rho \quad \equiv \ln(\text{DC}), \tag{7}$$

$$\text{polytropic index} \quad \equiv \quad n \quad \equiv \text{something near } \frac{5}{3}, \tag{8}$$

$$\text{and} \quad \text{dissipation number} \quad \equiv \quad \text{Di} \quad = \quad \frac{g_\text{o} H}{c_\text{p} \overline{T}_\text{o}}. \tag{9}$$

Here, $\overline{\rho}(r)$ is the background density and c_p is the constant-pressure specific heat.

If there is also a stable layer in the system (say, below the convection zone), some other parameters are needed: the transition location and width, along with the polytropic index of the stable layer or (if the stable layer isn't polytropic) the full entropy gradient $d\overline{S}/dr$ in the stable layer. For polytrope, n determines $d\overline{S}/dr$, with an order of magnitude of $[n/(5/3) - 1]c_\text{p}/r_\text{i}$. Regardless, the stable layer introduces an important, final dimensionless number:

$$\text{buoyancy parameter} \quad \equiv \quad \text{B} \quad \equiv \frac{\widetilde{N^2}}{\Omega_0^2}, \tag{10}$$

$$\text{where} \quad N^2 \equiv \frac{g}{c_\text{p}} \frac{d\overline{S}}{dr} \tag{11}$$

and the tilde indicates a volume average over the stable layer.

4 Christensen & Aubert (2006)

Christensen & Aubert (2006) explored saturated Boussinesq dynamos in the context of planetary magnetic fields

References

Brun, A. S., Strugarek, A., Noraz, Q., Perri, B., Varela, J., Augustson, K., Charbonneau, P., & Toomre, J. 2022, "Powering stellar magnetism: Energy transfers in cyclic dynamos of Sun-like stars", The Astrophysical Journal, 926, 21, doi: 10.3847/1538-4357/ac469b

Christensen, U. R., & Aubert, J. 2006, "Scaling properties of convection-driven dynamos in rotating spherical shells and application to planetary magnetic fields", Geophysical Journal International, 166, 97, doi: 10.1111/j.1365-246x.2006.03009.x

Christensen, U. R., Holzwarth, V., & Reiners, A. 2009, "Energy flux determines magnetic field strength of planets and stars", Nature, 457, 167, doi: 10.1038/nature07626

Guerrero, G., Zaire, B., Smolarkiewicz, P. K., de Gouveia Dal Pino, E. M., Kosovichev, A. G., & Mansour, N. N. 2019, "What sets the magnetic field strength and cycle period in solar-type stars?", The Astrophysical Journal, 880, 6, doi: 10.3847/1538-4357/ab224a

Jardine, M., & Unruh, Y. C. 1999, "Coronal emission and dynamo saturation", Astronomy & Astrophysics, 346, 883

Kraft, R. P. 1967, "Studies of stellar rotation. V. The dependence of rotation on age among solar-type stars", The Astrophysical Journal, 150, 551, doi: 10.1086/149359

Noyes, R. W., Hartmann, L. W., Baliunas, S. L., Duncan, D. K., & Vaughan, A. H. 1984, "Rotation, convection, and magnetic activity in lower main-sequence stars", The Astrophysical Journal, 279, 763, doi: 10.1086/161945

Pizzolato, N., Maggio, A., Micela, G., Sciortino, S., & Ventura, P. 2003, "The stellar activity-rotation relationship revisited: Dependence of saturated and non-saturated x-ray emission regimes on stellar mass for late-type dwarfs", Astronomy & Astrophysics, 397, 147, doi: 10.1051/0004-6361:20021560

Reiners, A., Shulyak, D., Käpylä, P. J., Ribas, I., Nagel, E., Zechmeister, M., Caballero, J. A., Shan, Y., Fuhrmeister, B., Quirrenbach, A., Amado, P. J., Montes, D., Jeffers, S. V., Azzaro, M., Béjar, V. J. S., Chaturvedi, P., Henning, T., Kürster, M., & Pallé, E. 2022, "Magnetism, rotation, and nonthermal emission in cool stars", Astronomy & Astrophysics, 662, A41, doi: 10.1051/0004-6361/202243251

Skumanich, A. 1972, "Time scales for Ca II emission decay, rotational braking, and lithium depletion", The Astrophysical Journal, 171, 565, doi: 10.1086/151310

Strugarek, A., Beaudoin, P., Charbonneau, P., Brun, A. S., & do Nascimento, J.-D. 2017, "Reconciling solar and stellar magnetic cycles with nonlinear dynamo simulations", Science, 357, 185, doi: 10.1126/science.aal3999

Walter, F. M. 1982, "On the coronae of rapidly rotating stars. III - an improved coronal rotation-activity relation in late type dwarfs", The Astrophysical Journal, 253, 745, doi: 10.1086/159675

Wright, N. J., Drake, J. J., Mamajek, E. E., & Henry, G. W. 2011, "The stellar-activity-rotation relationship and the evolution of stellar dynamos", The Astrophysical Journal, 743, 48, doi: 10.1088/0004-637x/743/1/48